

Geometry engineering for the RF behavior of low-dimensional gate-all-around transistors

A. Benali, F. L. Traversa, G. Albareda, M. Aghoutane * and X.Oriols
 Universitat Autònoma de Barcelona, 08193, Bellaterra, Spain
 * Universidad Abdelmalek Essaâdi, 93000, Tetuán, Morocco
 e-mail: abdelilah.benali@uab.es

INTRODUCTION

The RF characterization of nanostructure is a relevant issue for the modern and future electronic devices. However, theoretical predictions of their frequency dependent behavior is a very challenging task. Indeed, being nanoelectronic rapidly approaching Terahertz operating regimes, at such frequencies the electric current is not only controlled by the flux of electrons crossing a particular surface (conduction current), but also by the temporal variations of the electric field (displacement current). Since the electric field inside the active region device is strongly influenced by the device geometry, one can expect that these elements can have a strong influence on the displacement current and, in turn, on the RF behavior of the next-generation of nanoscale transistors.

HIGH-FREQUENCY NOISE DEPENDENCE ON THE DEVICE GEOMETRY

The direct computation of the time-dependent total (conduction and displacement) current accounts of numerical difficulties when implemented exploiting spatial grids and finite time-steps [1]. Alternatively, we will use the Ramo-Shockley-Pellegrini (RSP) theorems [2], [3], [4], which is free from these numerical limitations and provides an accurate relationship between the total current and the electron dynamics. Furthermore the RSP theorems can be extended to quantum system through Bohmian trajectories [1].

Analytical results

A single electron crossing the volume $L_x \times L_y \times L_z$ depicted in Fig. 1 is considered. The transport takes place along the x direction. Then, the total current in the surface S_1 can be defined through the RSP results reported in the expression (26) of Ref. [1]. We consider two limit cases: $L_x \ll L_y, L_z$ and $L_x \gg L_y, L_z$. The former has a total current $I_1(t)$

$$I_1(t) \approx \frac{|q|v_x}{L_x}, \quad (1)$$

while the latter reads

$$I_1(t) \approx |q|\alpha \cdot e^{\alpha(t-\tau)}, \quad (2)$$

The corresponding power spectral densities (PSDs) can be analytically computed for both geometries. In Fig. 2, we plot the results $PSD_1(\omega)$ for a channel with a longitudinal dimension L_x larger than the lateral ones (blue squares line) and, $PSD'_1(\omega)$ for the contrary (black circles line).

Monte Carlo results

In order to confirm previous results, we have carried out simulations of the total current using a many-particle Monte Carlo simulator named BITLLES that employs either classical or Bohmian (quantum) trajectories [5], [6]. The BITLLES simulator is able to calculate the time-dependent current in electronic devices by including the self-consistent solution of electron transport and Poisson equations, beyond the standard mean-field approximation [7]. In particular, the noise spectrum of a gate-all-around Silicon nanowire (which is a typical multigate structure avoiding short-channel effects with a low-dimensional channel to reach higher mobilities) has been simulated. In Fig. 3, the numerical power spectral densities for three different geometries are reported confirming the simpler analytical results.

Understanding the results

For a two terminal device, the lines of the electric field leaving through surfaces S_2, S_3, S_5 and S_6 of Fig. 1 will finally end at one of the two terminals. Thus, the current in the drain terminal is not due to the time-dependent electric field on S_1 alone. However, for the gate-all-around transistor considered here, the current at the drain terminal is roughly equal to the time-dependent electric field on S_1 . thus, a moving electron inside the channel generates a time-dependent field on S_1 . The displacement current on that surface is inversely proportional to the electron-surface distance and proportional to S_1 . Thus, an electron traversing the transistor with smaller lateral area will generate a sharper pulse on drain terminal, i.e. on the surface S_1 , as seen in the subplot (c) of Fig. 5. An equivalent explanation is furnished by the RSP theorem. The current pulse on the S_1 depends on the functions $\phi_1(\vec{r})$ and $\vec{F}_1(\vec{r})$ (see expression (20) in Ref. [1]). Since, by definition $\phi_1(\vec{r})$ and $\vec{F}_1(\vec{r})$ depends on the geometry (Fig. 4), the current pulses do also depend on it (Fig. 5).

CONCLUSION

Analytical and numerical results show that, for gate-all-around transistors, the frequency range of the high-frequency noise increases, when the ratio longitudinal/transversal dimensions increases. In the conference, similar results for the s-parameters, f_T and f_{max} will be presented. In the transistors discussed here, the intrinsic RF spectrum does not longer depend on the transit time of the electron along the channel, but mainly on the channel geometry.

ACKNOWLEDGMENT

This work has been partially supported through MEC project MICINN TEC2009-06986 and by AECID.

REFERENCES

[1] A. Alarcón and X. Oriols, Journal of Statistical Mechanics: Theory and Experiment. 2009, P01051 (2009).
 [2] S. Ramo, Proceedings of the I. R. E. , 27, 584 (1939).
 [3] W. Shockley, J. Appl. Phys. 9, 635 (1938).
 [4] B. Pellegrini, Physical Review B, 34(8), 5921 (1986).
 [5] http://europa.uab.es/bitlles
 [6] X. Oriols, Phys. Rev. Lett. 98 (2007) 066803.
 [7] G. Albareda, J. Suñé and X. Oriols, Phys. Rev. B, 79(7) (2009) 075315.

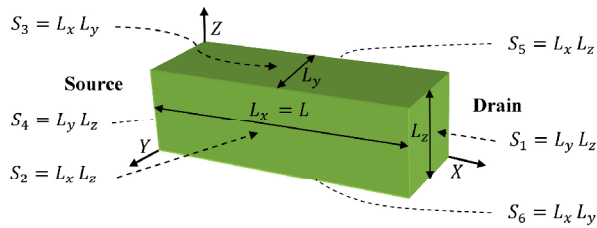


Fig. 1. Schematic representation of an arbitrary parallelepiped representing the a channel region of a gate-all-around transistor. The channel has dimensions L_x, L_y, L_z and it is limited by the closed surface $S = \{S_1, S_2, \dots, S_6\}$. Transport takes place from source to drain.

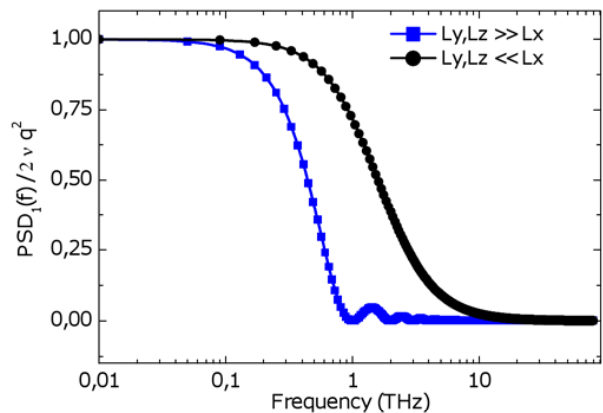


Fig. 2. Power spectral density $PSD(f)$ (in units of $2q^2\nu$, ν is the injection rate) for the analytical current defined in (1) (blue squares) and (2) (black circles). A constant velocity $v_x = 10^5$ m/s. is assumed on those analytical expressions. Coulomb correlations are ignored.

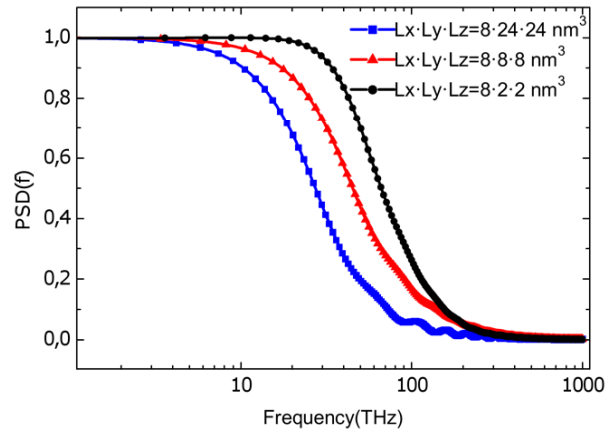


Fig. 3. Monte Carlo numerical results for the power spectral density $PSD(f)$ of three different geometries of the gate-all-around quantum-wire transistor described in the text. Full coulomb correlations (beyond the mean-field approximation) are considered.

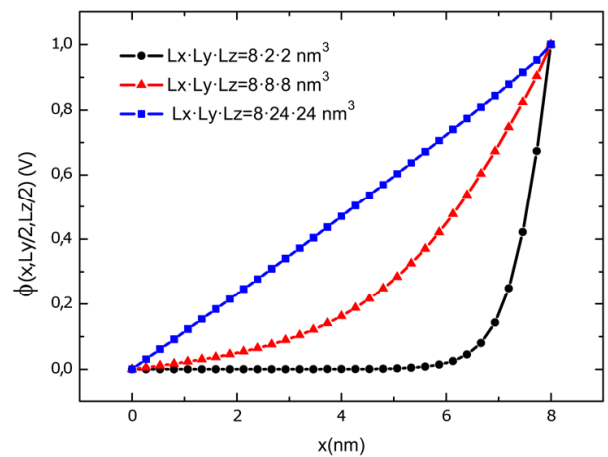


Fig. 4. Representation of $\phi_1(\vec{r})$ (without units) for the three particular geometries of the gate-all-around transistor discussed in Fig. 3.

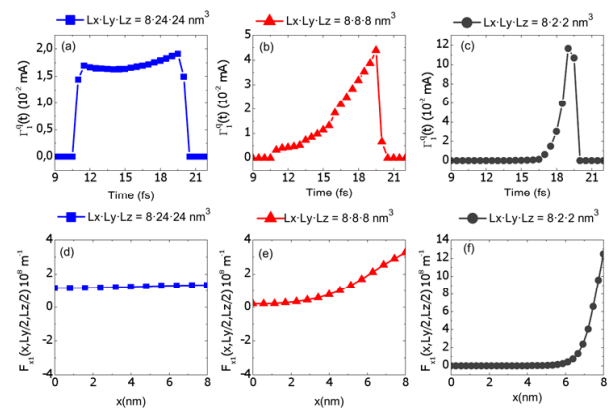


Fig. 5. (a), (b) and (c), numerical self-consistent contribution of one trajectory in the current $I_1(t)$ of a gate-all-around transistor with the three different geometries discussed in the text. (d), (e) and (f), numerical computation of the function $F_1(\vec{r})$ (see [1] for its definition) in the transport direction for the three geometries.